Current Biology 22, 956–966, June 5, 2012 ©2012 Elsevier Ltd All rights reserved DOI 10.1016/j.cub.2012.03.068

Article

PTK7 Regulates Myosin II Activity to Orient Planar Polarity in the Mammalian Auditory Epithelium

Jianyi Lee,[1] Anna Andreeva,[1] Conor W. Sipe,[1] Lixia Liu,[1,2] Amy Cheng,[1,3] and Xiaowei Lu[1,*]
[1]Department of Cell Biology, P.O. Box 800732, University of Virginia, Charlottesville, VA 22908, USA

Summary

Background: Planar cell polarity (PCP) signaling is a key regulator of epithelial morphogenesis, including neural tube closure and the orientation of inner ear sensory hair cells, and is mediated by a conserved noncanonical Wnt pathway. *Ptk7* is a novel vertebrate-specific regulator of PCP, yet the mechanisms by which *Ptk7* regulates mammalian epithelial PCP remain poorly understood.
Results: Here we show that, in the mammalian auditory epithelium, *Ptk7* is not required for membrane recruitment of Dishevelled 2; *Ptk7* and *Frizzled3*/*Frizzled6* receptors act in parallel and have opposing effects on hair cell PCP. Mosaic analysis identified a requirement of *Ptk7* in neighboring supporting cells for hair cell PCP. *Ptk7* and the noncanonical Wnt pathway differentially regulate a contractile myosin II network near the apical surface of supporting cells. We provide evidence that this apical myosin II network exerts polarized contractile tension on hair cells to align their PCP, as revealed by asymmetric junctional recruitment of vinculin, a tension-sensitive actin binding protein. In *Ptk7* mutants, compromised myosin II activity resulted in loss of planar asymmetry and reduced junctional localization of vinculin. By contrast, vinculin planar asymmetry and stereociliary bundle orientation were restored in $Fz3^{-/-};Ptk7^{-/-}$ double mutants.
Conclusions: These findings suggest that PTK7 acts in conjunction with the noncanonical Wnt pathway to orient epithelial PCP through modulation of myosin II-based contractile tension between supporting cells and hair cells.

Introduction

Epithelial cells are often polarized within the plane of a cell sheet, perpendicular to the apical-basal polarity axis. One of the most prominent examples of epithelial planar cell polarity (PCP) is found in the mammalian auditory sensory epithelium, the organ of Corti (OC). The OC is composed of one row of inner hair cells (IHC) and three rows of outer hair cells (OHC) and nonsensory supporting cells. Hair cells are separated from one another by supporting cells, forming a checkerboard pattern. The stereociliary bundle, the mechanotransduction organelle located on the apical surface of the hair cell, consists of rows of actin-based stereocilia of graded heights in a V-shaped array. This structural asymmetry of the stereociliary bundle defines PCP of an individual hair cell. Across the OC, hair cells display uniform planar polarity, with the vertex of their V-shaped stereociliary bundles all pointing to the lateral edge of the cochlear duct. Uniform bundle orientation is required for normal sound perception [1].

Inner ear PCP is regulated by an evolutionarily conserved noncanonical Wnt pathway, which has emerged as a key regulator of metazoan tissue morphogenesis, including convergent extension (CE) movements during axis elongation, neural tube closure, and inner ear morphogenesis [2]. The core components of the noncanonical Wnt pathway are Frizzled (Fz), Dishevelled (Dsh/Dvl), Strabismus (Stbm)/Van Gogh (Vang), Starry night (Stan)/Flamingo (Fmi), Diego (Dgo), and Prickle (Pk). These molecules engage in both intra- and intercellular signaling to align PCP in neighboring cells. In other systems, members of the Rho family small GTPases (RhoA, Rac1, and Cdc42) and their effectors, including Rho-associated kinases (ROCK) and c-Jun N-terminal kinases (JNK), have been implicated in PCP signaling downstream of the core components. In the inner ear, the noncanonical Wnt pathway is required for stereociliary bundle orientation and cochlear convergent extension [3]. Mutations in homologs of Fmi (Celsr1), Vang (Vangl1/Vangl2), Fz (Fz2/Fz3/Fz6), and Dsh (Dvl1/Dvl2/Dvl3) cause misoriented stereociliary bundles and a shortened cochlear duct [2]. The small GTPase Rac1 and its downstream effector p21-activated kinases (PAK) regulate hair cell PCP in the OC [4, 5], and nonmuscle myosin II has been implicated in cochlear extension [6].

In addition to the conserved noncanonical Wnt pathway, novel PCP regulators have been identified in mammals, including protein tyrosine kinase 7 (*Ptk7*), a receptor tyrosine kinase-like molecule [7–11]. Mouse *Ptk7* mutations cause similar phenotypes to those of noncanonical Wnt pathway mutants, including neural tube and hair cell PCP defects [8, 12]. In *Xenopus*, *Ptk7* has been shown to regulate neural tube closure [8] and neural crest migration [13, 14] by mediating membrane recruitment of Dishevelled through PKCδ and the adaptor molecule RACK1 [13, 14]. However, it is unclear whether PTK7 regulates mammalian epithelial PCP by a similar mechanism, because PTK7 has been shown to mediate mesodermal CE in mice without affecting Dvl2 membrane localization [15].

To gain insight into the mechanisms by which PTK7 regulates mammalian epithelial PCP, we carried out a functional dissection of *Ptk7* in planar polarization of hair cells in the OC, where bundle orientation provides a robust and quantifiable readout for PCP at single-cell resolution. Our results reveal that *Ptk7* and the noncanonical Wnt pathway differentially regulate myosin II-based contractility to align hair cell PCP. We show that *Ptk7* is required in supporting cells to orient hair cell PCP, probably by exerting contractile tension on neighboring hair cells through an apical myosin II network.

Results

Ptk7 Is Not Required for Asymmetric Membrane Localization of Dishevelled 2 in the OC

Membrane recruitment and asymmetric localization of the cytoplasmic scaffold protein Dishevelled is a conserved

[2]Present address: Department of Medicine, Allergy and Immunology, P.O. Box 800133, University of Virginia, Charlottesville, VA 22908, USA
[3]Present address: Georgetown University School of Medicine, Washington, DC 20057, USA
*Correspondence: xl6f@virginia.edu

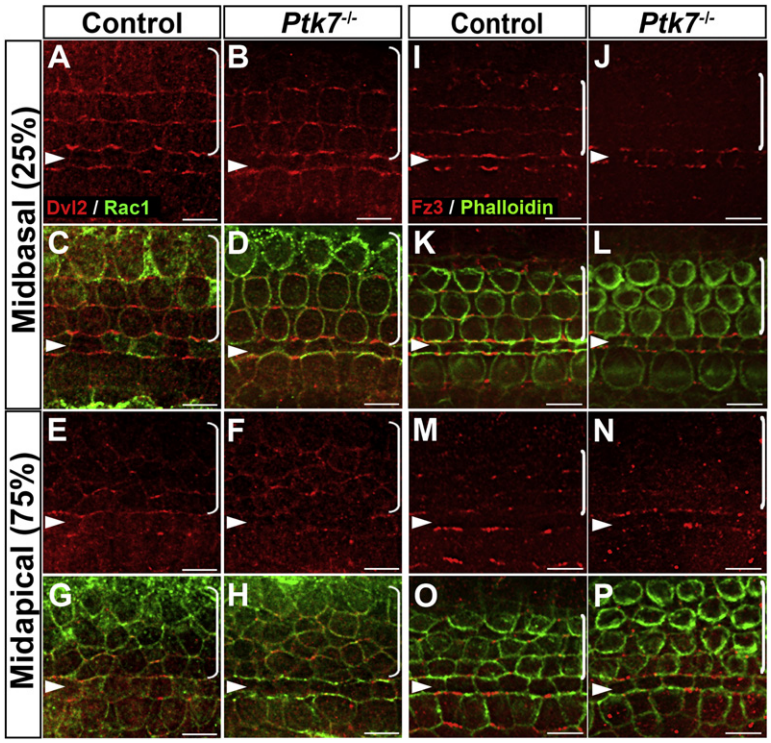

Figure 1. *Ptk7* Regulates Fz3 Localization but Is Not Required for Asymmetric Localization of Dvl2 in the OC

(A–D) In the midbasal region of the OC at E17.5, Dvl2 (red) was enriched on the lateral membranes of hair cells in both control (A, C) and $Ptk7^{-/-}$ (B, D) cochleae.

(E–H) In the midapical region of the OC at E17.5, similar membrane localization of Dvl2 was observed in control (E, G) and $Ptk7^{-/-}$ (F, H) cochleae. Cell boundaries were labeled with Rac1 immunostaining (green).

(I–L) In the midbasal region of OC at E17.5, Fz3 (red) was enriched on the medial membranes of hair cells and supporting cells in the control (I, K). This localization was disrupted in $Ptk7^{-/-}$ cochleae (J, L).

(M–P) In the midapical region of the OC at E17.5, asymmetric localization of Fz3 was not apparent in either control (M, O) or $Ptk7^{-/-}$ (N, P) cochleae.

Green, phalloidin staining. Percentages indicate the distance of the positions analyzed from the base relative to the length of the cochlea. Arrowheads indicate the row of pillar cells. Brackets indicate OHC rows. Lateral is up in all micrographs. Scale bars represent 6 μm. See also Figure S1.

readout for PCP signaling [16–18]. To determine where *Ptk7* intersects with the noncanonical Wnt pathway, we first tested whether *Ptk7* is required for membrane recruitment of Dvl2. At E17.5, in the midbasal region of control OC, endogenous Dvl2 is asymmetrically localized and appears to be enriched on the lateral membranes of hair cells (Figures 1A and 1C). Dvl2 localization is disrupted in $Vangl2^{Lp/Lp}$ OC [18] and $Fz3^{-/-}$; $Fz6^{-/-}$ OC (Figure S1 available online), indicating that Dvl2 localization is a functional readout of the noncanonical Wnt pathway activity. By contrast, Dvl2 localization was normal in the $Ptk7^{-/-}$ OC at E17.5 (Figures 1B and 1D). Similarly, in the midapical region of OC, membrane recruitment of Dvl2 occurred in both control and $Ptk7^{-/-}$ OC (Figures 1E–1H). We also examined Fz3 localization at E17.5, which is normally enriched along the medial poles of hair cells and supporting cells [19, 20] (Figures 1I, 1K, 1M, and 1O). Interestingly, membrane localization of Fz3 was significantly reduced in the $Ptk7^{-/-}$ OC (Figures 1J, 1L, 1N, and 1P). These results indicate that *Ptk7* regulates Fz3 localization but is not required for asymmetric membrane localization of Dvl2 in the OC. Thus, the noncanonical Wnt pathway is at least partially active in the absence of *Ptk7*.

PTK7 and Fz3/Fz6 Receptors Act in Parallel and Have Opposing Effects on Hair Cell PCP

The normal Dvl2 membrane localization and reduced Fz3 localization in $Ptk7^{-/-}$ OC suggests that *Ptk7* is not an obligatory component of the noncanonical Wnt pathway, but it may regulate the strength of noncanonical Wnt signaling. To test this idea, we next sought to determine the epistatic relationship between *Ptk7* and the *Fz3/Fz6* genes. Mouse *Fz3* and *Fz6* regulate PCP signaling in a redundant manner [19]. We used bundle orientation as readout for PCP, which is already evident at embryonic day (E) 18.5. In the control, the vertices of the V-shaped stereociliary bundles all point toward the lateral edge of the cochlear duct (Figures 2A and 2A′). Whereas *Fz3* or *Fz6* single mutants had normal bundle orientation (Figures 2B and 2B′ and data not shown), $Fz3^{-/-}$;$Fz6^{-/-}$ mutants had misoriented stereociliary bundles, affecting primarily IHCs [19] (Figures 2C, 2C′, and S2). By contrast, in the $Ptk7^{-/-}$ OC, bundle misorientation was confined to OHC3 (Figures 2D, 2D′, and S2). Surprisingly, bundle misorientation in OHC3 was significantly suppressed in both $Fz3^{-/-}$;$Ptk7^{-/-}$ and $Fz6^{-/-}$; $Ptk7^{-/-}$ mutants (Figures 2E and 2E′ and data not shown). These results indicate that *Ptk7* and *Fz3/Fz6* have opposing effects on hair cell PCP and suggest that *Ptk7* acts upstream of or in parallel to *Fz3/Fz6*. To distinguish between these two possibilities, we analyzed bundle orientation in $Fz3^{-/-}$; $Fz6^{-/-}$;$Ptk7^{-/-}$ triple mutants. If *Ptk7* acts upstream of *Fz3/Fz6* in a linear genetic pathway, then the *Fz* mutations should be epistatic to *Ptk7*, i.e., the triple mutants should have a phenotype similar to *Fz3/Fz6* double mutants. On the other hand, if *Ptk7* acts in parallel to *Fz3/Fz6*, then neither mutation should be epistatic; instead, the triple mutants may show an additive phenotype. Indeed, the triple mutants displayed a combination of the *Fz3/Fz6* and *Ptk7* mutant phenotypes: both IHC and OHC rows displayed misoriented stereociliary bundles (Figures 2F, 2F′, and S2). Taken together, these results indicate that *Ptk7* and *Fz3/Fz6* act in parallel and have opposing effects on hair cell PCP.

Ptk7 Is Required in Supporting Cells to Regulate Hair Cell PCP

Next, we sought to determine the site of action of *Ptk7* in the OC. To this end, we generated a "floxed" allele of *Ptk7* ($Ptk7^{CO}$). A knockout allele ($Ptk7^{-}$) was derived from $Ptk7^{CO}$ upon germline Cre expression (Figures S3A and S3B). We first used the $Foxg1^{Cre}$ line [21] to inactivate *Ptk7* in the entire cochlear epithelium. OHC3s in these mutants displayed misoriented stereociliary bundles similar to $Ptk7^{-/-}$ mutants (Figures S3C–S3E), indicating that *Ptk7* acts within the cochlear epithelium to regulate hair cell PCP.

We then carried out genetic mosaic analysis to further determine the cell type-specific requirement of *Ptk7*. PTK7 is expressed in both hair cells and supporting cells and colocalizes with the adherens junction protein E-cadherin [8] (Figure 3B).

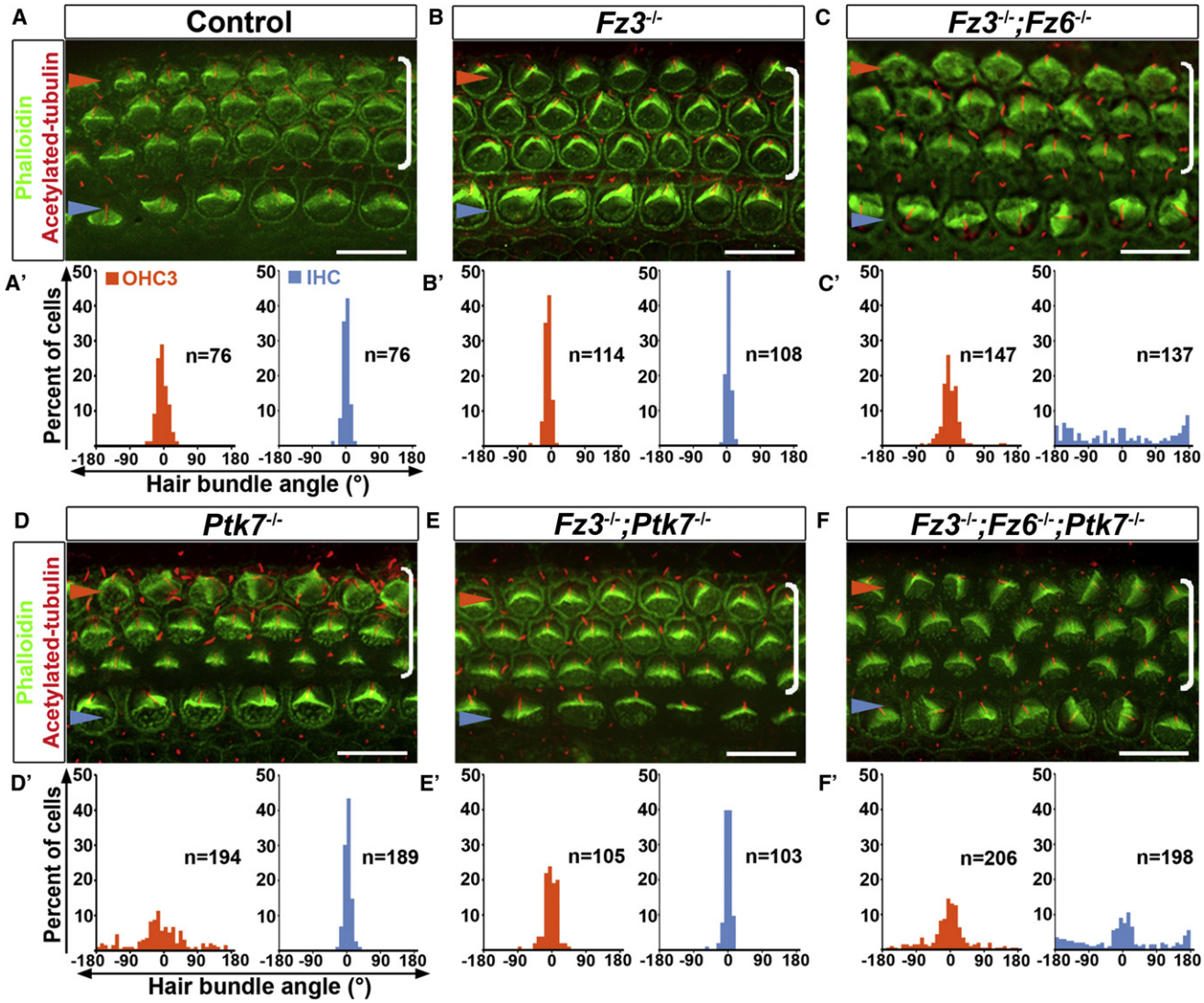

Figure 2. Epistasis Analysis of *Ptk7* and *Fz3/Fz6* in Hair Cell PCP

(A–F) Basal region (15% cochlear length) of E18.5 cochleae stained with phalloidin (green) and acetylated tubulin (red) to visualize the stereocilia and the kinocilium, respectively. Genotypes are indicated above the panels.

(A′–F′) Quantification of bundle orientation in OHC3 (orange bars) and IHC (blue bars) rows for the indicated genotypes.

(A and B) In control (A, A′) and $Fz3^{-/-}$ (B, B′) cochleae, OHC3 and IHC bundle orientation do not deviate beyond 30° from the medial-lateral axis.

(C and C′) In $Fz3^{-/-}$;$Fz6^{-/-}$ mutants, the bundle orientation defect was most pronounced in IHCs.

(D and D′) In $Ptk7^{-/-}$ mutants, bundle orientation defects were most pronounced in OHC3s.

(E and E′) In $Fz3^{-/-}$;$Ptk7^{-/-}$ mutants, bundle orientation in OHC3s was significantly improved compared to $Ptk7^{-/-}$ mutants.

(F and F′) $Fz3^{-/-}$;$Fz6^{-/-}$;$Ptk7^{-/-}$ triple mutants displayed an additive defect in bundle orientation.

Blue arrowheads indicate the row of IHCs, orange arrowheads indicate the OHC3 row, and brackets indicate all OHC rows. Lateral is up in all micrographs. Scale bars represent 10 μm. See also Figure S2.

To generate *Ptk7* mosaics, we took advantage of the *Ella-Cre* line [22], which expresses Cre in all cells but at variable levels. In *Ella-Cre; Ptk7*$^{CO/-}$ animals, cells with high Cre expression level would have a genotype of $Ptk7^{-/-}$, whereas cells with low Cre expression level would have a genotype of $Ptk7^{CO/-}$, thus retaining a functional copy of *Ptk7* (referred to as $Ptk7^{+}$ thereafter). The genotypes of individual cells in the OC were unambiguously determined by the presence or absence of PTK7 immunostaining (Figures 3B–3F). Because only OHC3s were affected in *Ptk7* mutants, we focused on OHC3s and correlated bundle orientation with the genotypes of each hair cell and its four immediate supporting cell neighbors (Figure 3A, shaded in blue). Many mosaics had a $Ptk7^{+}$ hair cell with a misoriented stereociliary bundle surrounded by varying numbers of $Ptk7^{-/-}$ supporting cells (arrows, Figures 3C–3F″). Moreover, as the number of $Ptk7^{-/-}$ supporting cells surrounding a $Ptk7^{+}$ hair cell increased (up to four), both the penetrance and the severity of bundle misorientation defect increased (Figures 3G and 3H). Together, these results indicate that *Ptk7* function in hair cells alone is insufficient for normal bundle orientation and that *Ptk7* is required in supporting cells to regulate hair cell PCP.

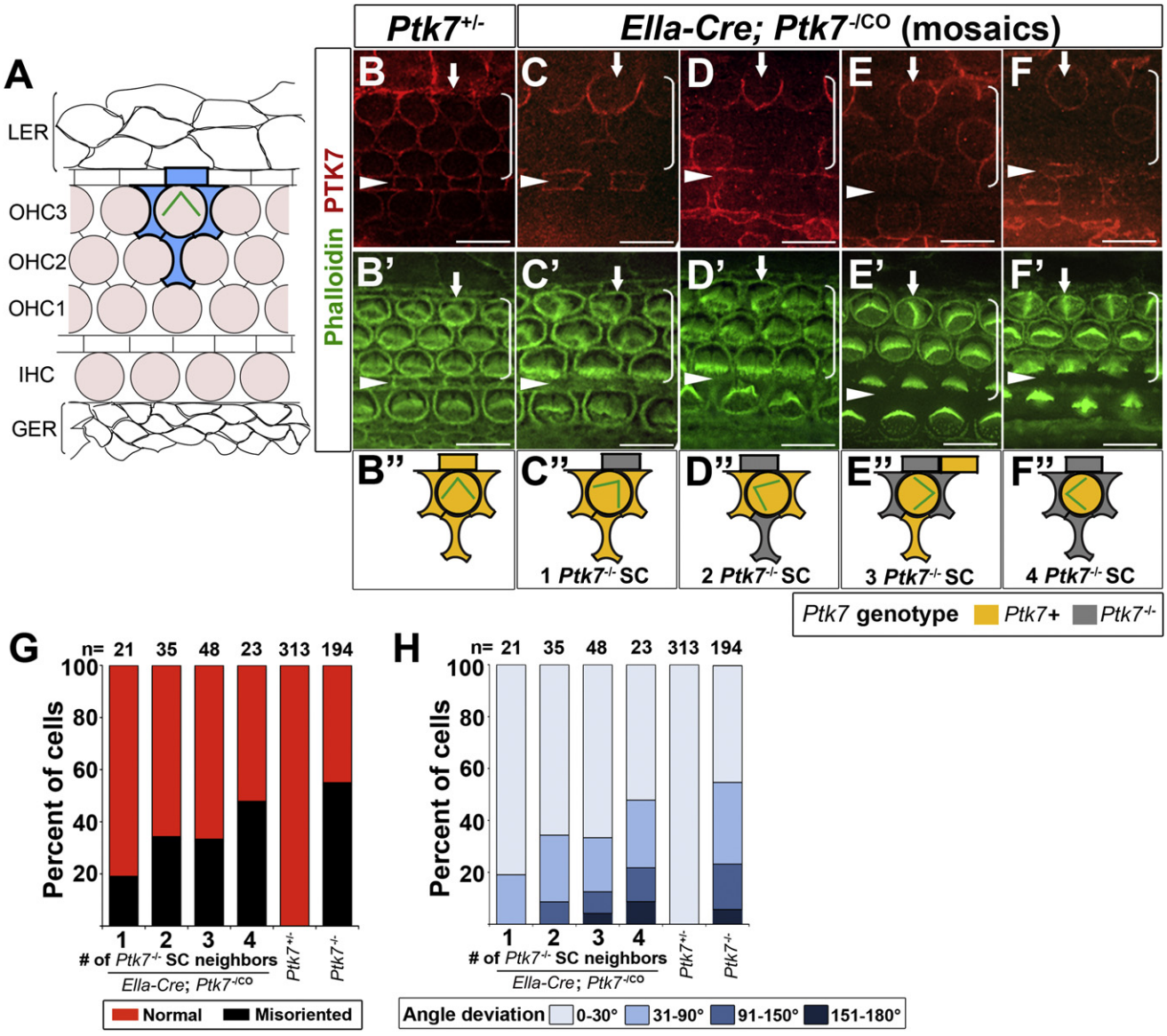

Figure 3. Mosaic Analysis of *Ptk7* in Hair Cell PCP

(A) Schematic diagram of cellular organization in the OC. Hair cells (shaded light pink) are separated from one another by intervening supporting cells. Each hair cell in OHC3 is immediately surrounded by four supporting cells (shaded in blue). Flanking the OC are cells of the lesser epithelial ridge (LER) and the greater epithelial ridge (GER).

(B–F″) Midbasal region (25% cochlear length) of E18.5 cochleae stained with PTK7 antibodies (red) and phalloidin (green).

(B and B′) In controls, PTK7 is expressed in both hair cells and supporting cells and localized to cell-cell contacts.

(C–F″) Examples of *Ptk7* mosaics in *Ella-Cre; Ptk7*$^{-/CO}$ cochleae. Ptk7^{+} hair cells with misoriented stereociliary bundles (arrows) surrounded by different numbers of *Ptk7*$^{-/-}$ supporting cells (SC) are shown and schematized.

(G and H) In *Ella-Cre; Ptk7*$^{-/CO}$ mosaic cochleae, both the penetrance (G) and the severity (H) of bundle orientation defects in Ptk7^{+} OHC3 positively correlates with the number of *Ptk7*$^{-/-}$ supporting cell neighbors.

Arrowheads indicate the row of pillar cells. Brackets indicate OHC rows. Lateral is up in all micrographs. Scale bars represent 10 μm. See also Figure S3.

JNK Signaling Is Unlikely to Mediate PTK7 Function in the OC

Our results so far are consistent with a model where *Ptk7* and the noncanonical Wnt pathway converge on common effectors to regulate bundle orientation. It has been shown that the noncanonical Wnt pathway activates JNK signaling in other systems [23, 24]. We therefore considered the possibility that *Ptk7* has an opposing effect on Fz-mediated JNK signaling. To test this, we performed biochemical assays for JNK activation in HEK293T cells (Figure 4A). Using phosphorylation of c-Jun as readout, we found that expression of PTK7 alone had a minimal effect on JNK activation, while expression of Fz3 alone led to JNK activation. Moreover, coexpression of PTK7 and Fz3 did not inhibit JNK activation by Fz3. Thus, in this heterologous system, there was no apparent effect of PTK7 on JNK signaling.

Next, we examined whether PTK7 regulates JNK signaling in vivo. By using antibodies that specifically recognize

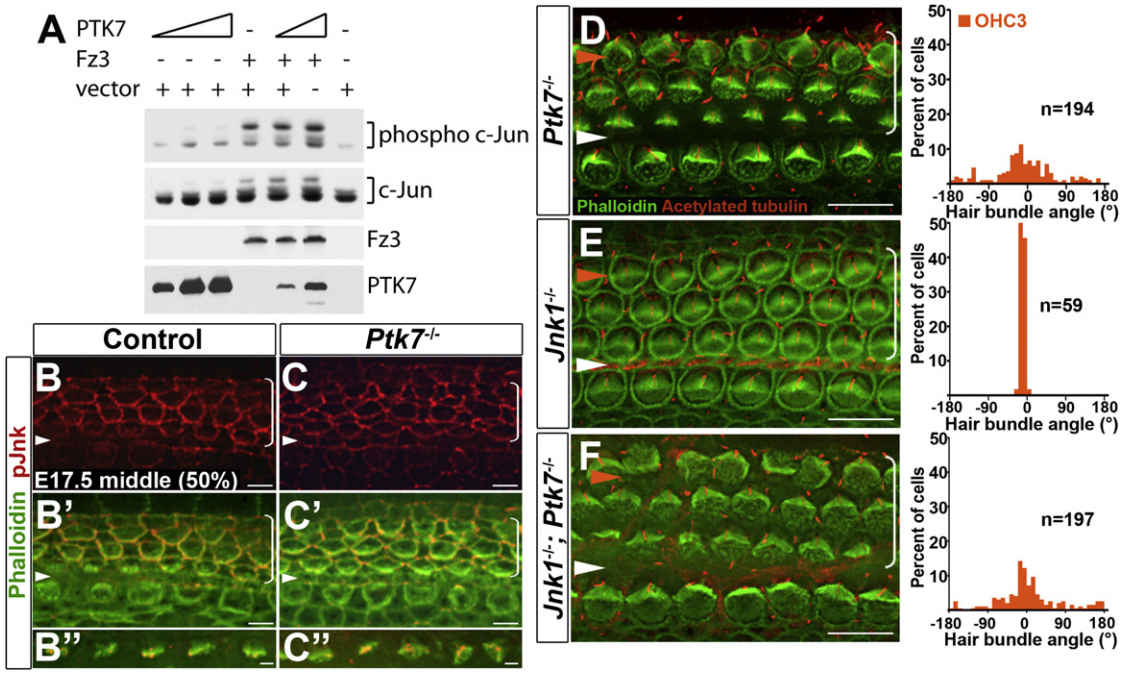

Figure 4. JNK Signaling Is Unlikely to Mediate PTK7 Function in the OC

(A) PTK7 expression has no effect on JNK activation in vitro. HEK293T cells were transfected either with PTK7, Fz3, or both and assayed for c-Jun phosphorylation.

(B–C″) In the middle turn of E17.5 OC (50% cochlear length), pJNK localization (red) in the *Ptk7*$^{-/-}$ OC (C–C″) was similar to the control (B–B″). Green, phalloidin staining.

(D–F) Basal region (15% cochlear length) of E18.5 *Ptk7*$^{-/-}$ (D), *Jnk1*$^{-/-}$ (E), and *Jnk1*$^{-/-}$;*Ptk7*$^{-/-}$ (F) cochleae stained with phalloidin (green) and acetylated tubulin (red). Quantifications of bundle orientation of OHC3s are shown to the right.

White arrowheads indicate the row of pillar cells; orange arrowheads indicate the OHC3 row. Brackets indicate OHC rows. Lateral is up in all micrographs. Scale bars represent 6 μm in (B)–(C′), 2 μm in (B″) and (C″), and 10 μm in (D)–(F).

phosphorylated and activated JNK (pJNK), we found that in E17.5 controls, pJNK localized to cellular junctions and the tips of a subset of stereocilia (Figures 4B–4B″), suggesting that JNK signaling is active during cochlear morphogenesis. However, in *Ptk7*$^{-/-}$ OC, we did not observe any significant changes in pJNK levels or localization (Figures 4C–4C″), suggesting that JNK is unlikely to be a downstream effector of PTK7 in the OC.

To more rigorously assess whether PTK7 regulates inner ear PCP through JNK signaling, we next examined genetic interactions between *Ptk7* and the *Jnk* genes by using bundle orientation as readout. Among the three mouse homologs of Jnk, *Jnk1* and *Jnk2* are broadly expressed. Although single *Jnk* knockout mice are viable, *Jnk1*/*Jnk2* double mutants display neural tube defects and die at E10.5 [25–27]. We found that *Jnk1* and *Jnk2* single mutants had essentially normal bundle orientation at E18.5 (Figure 4E and data not shown). In the *Jnk1*$^{-/-}$;*Ptk7*$^{-/-}$ OC, bundle misorientation persisted in OHC3s, comparable in severity to *Ptk7*$^{-/-}$ mutants (Figure 4F). Similar results were obtained in *Jnk2*$^{-/-}$;*Ptk7*$^{-/-}$ double mutants (data not shown). Therefore, unlike *Fz3*/*Fz6* mutations, *Jnk1*/*Jnk2* mutations had no effect on the bundle misorientation phenotype of *Ptk7* mutants, providing further evidence that JNK is unlikely to mediate PTK7 signaling in the OC.

Ptk7 and the Noncanonical Wnt Pathway Differentially Regulate a Contractile Apical Myosin II Network in Supporting Cells

To further pursue downstream effectors of *Ptk7*, we next investigated a potential role of *Ptk7* in regulating myosin II function in the OC. It has been shown that noncanonical Wnt signaling activates actomyosin contractility in other systems [28–30]. Moreover, myosin II regulates CE and neural tube closure in *Xenopus* [31, 32] and cochlear extension in mice [6].

We first examined myosin IIB (MIIB, encoded by *Myh10*), one of the three myosin II heavy chain proteins (MIIA, MIIB, and MIIC) expressed during cochlear morphogenesis [6]. Hair cell planar polarization and stereociliary bundle formation proceed in a base-to-apex gradient starting at the base of the cochlea around E16.5, as evidenced by migration of the axonemal kinocilium [7] and asymmetric localization of activated PAK [4]. At E16.5, in control tissues, MIIB was localized to cellular junctions [6] (Figures 5A–5E). In addition, in the midbasal region of the cochlea, we also observed an assembly of MIIB foci near the apical surface of supporting cells (pillar and Deiters' cells) (Figures 5A–5C, arrows). By contrast, the apical MIIB foci were absent from the supporting cells in the midbasal region of the *Ptk7*$^{-/-}$ OC, and overall junctional localization of MIIB was reduced compared to controls (Figures 5F–5J). Western blot analysis of E16.5 cochlear lysates showed that total levels of MIIB in *Ptk7*$^{-/-}$ cochleae were similar to controls (Figure 5K). These results indicate that *Ptk7* promotes junctional localization of MIIB and is required for the assembly of apical MIIB foci in supporting cells.

To determine whether the noncanonical Wnt pathway also regulates MIIB localization, we examined *Fz3*$^{-/-}$;*Fz6*$^{-/-}$ and *Vangl2*$^{Lp/Lp}$ cochleae at E16.5. In contrast to *Ptk7* mutants, the apical MIIB foci still formed in the supporting cells of *Fz3*$^{-/-}$;*Fz6*$^{-/-}$ and *Vangl2*$^{Lp/Lp}$ mutants, albeit smaller in size compared to controls (Figures 5L–5O). Interestingly, junctional

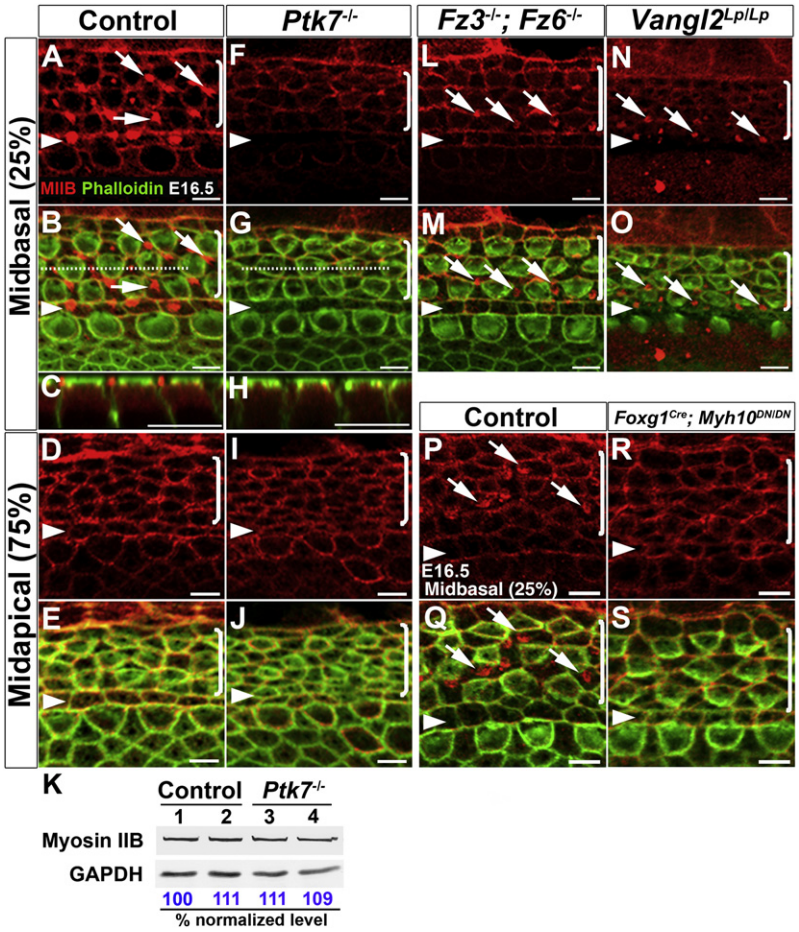

Figure 5. *Ptk7* and the Noncanonical Wnt Pathway Differentially Regulate a Contractile Myosin IIB Network in Supporting Cells

(A–J, L–S) Confocal images of MIIB (red) and phalloidin (green) staining in the OC at E16.5.

(A–E) In the control OC, MIIB is localized to cell-cell contacts and to apical foci in the supporting cells in the midbasal region of the OC (A–C).

(F–J) In *Ptk7*$^{-/-}$ OC, apical MIIB foci were absent from supporting cells (F–H) and overall junctional MIIB staining was reduced.

(C and H) Z projections along the dashed lines in (B) and (G), respectively, showing the apical position of the MIIB foci in supporting cells.

(K) Total levels of MIIB in E16.5 *Ptk7*$^{-/-}$ cochleae were comparable to controls. Lysates from four cochleae of the same genotype were pooled and loaded in each lane. GAPDH served as loading control. Numbers on the bottom indicate percentage of normalized levels.

(L–O) Apical MIIB foci (arrows) were still present in the supporting cells of *Fz3*$^{-/-}$;*Fz6*$^{-/-}$ (L, M) and *Vangl2*$^{Lp/Lp}$ (N, O) mutants, albeit smaller in size.

(P and Q) Wild-type MIIB is localized to cell-cell contacts and apical foci in supporting cells (arrows).

(R and S) ATPase-deficient MIIB (R709C) was localized to cell-cell contacts but failed to assemble into apical foci in supporting cells.

Percentages indicate the distance of the positions analyzed from the base relative to the length of the cochlea. Arrowheads indicate the row of pillar cells. Brackets indicate OHC rows. Lateral is up in all micrographs. Scale bars represent 5 μm.

MIIB levels were significantly reduced in *Vangl2*$^{Lp/Lp}$ mutants (Figures 5N and 5O) but only slightly reduced in *Fz3*$^{-/-}$; *Fz6*$^{-/-}$ mutants (Figures 5L and 5M). Thus, *Ptk7* and the noncanonical Wnt pathway differentially regulate MIIB localization in the OC.

We next asked whether the apical MIIB foci in supporting cells were contractile structures. Because force generation by myosin II molecules requires their ATPase activity [33], we reasoned that formation of an active contractile network should be disrupted upon inhibition of the myosin ATPase activity. To test this hypothesis, we took advantage of a Cre-inducible dominant-negative allele of *Myh10* (*Myh10*^{DN}) carrying a point mutation (R709C) in MIIB, which retains actin binding but compromises the actin-activated ATPase activity [34]. *Foxg1*^{Cre} was used to activate the expression of MIIB (R709C) in the cochlear epithelium, such that *Foxg1*^{Cre};*Myh10*$^{DN/DN}$ animals expressed only mutant (R709C) MIIB in the cochlea. Immunostaining revealed that MIIB (R709C) was still localized to cellular junctions but failed to assemble into apical foci in supporting cells at E16.5 (Figures 5R and 5S). These observations indicate that assembly of apical MIIB foci requires its ATPase activity and strongly suggest that the apical MIIB foci in supporting cells are contractile structures.

Ptk7 Regulates Myosin II Activity to Orient Hair Cell PCP

Decreased junctional MIIB level and the absence of apical MIIB foci in the *Ptk7*$^{-/-}$ OC suggest compromised myosin II activity. Myosin II is activated by myosin regulatory light chain (RLC) phosphorylation, which is required for actomyosin contractility [33]. We therefore examined the distribution of phosphorylated RLC (pRLC) in the OC. At E16.5, in the midbasal region of the control OC, pRLC was primarily detected at cellular junctions with higher intensity around pillar cell membranes (Figures 6A and 6B). In E16.5 *Ptk7*$^{-/-}$ OC, pRLC staining appeared to be decreased at cell-cell contacts compared to controls, but, surprisingly, it was highly localized to apical foci in supporting cells (Figures 6C and 6D, arrows). By western blot analysis, *Ptk7*$^{-/-}$ cochleae showed a ~2-fold increase in total pRLC levels compared to controls (Figure 6M).

The paradox of the absence of MIIB and increased staining of pRLC in apical foci in *Ptk7*$^{-/-}$ supporting cells suggests that other myosin II heavy chain molecules may be present in these structures. We therefore examined MIIC and MIIA distribution in *Ptk7*$^{-/-}$ OC. In the midbasal region of the control OC at E16.5, both MIIC and MIIA were detected at apical foci in supporting cells (Figures 6E, 6F, 6I, and 6J). Overall, MIIC appeared to be enriched in supporting cells, whereas MIIA localization was diffused and hardly detectable at cell boundaries. In *Ptk7*$^{-/-}$ OC, MIIC staining appeared to be decreased at cell-cell contacts but was still present at apical foci in supporting cells (Figures 6G and 6H), whereas MIIA staining at apical foci in supporting cells was greatly reduced (Figures 6K and 6L). Western blot analysis showed that in *Ptk7*$^{-/-}$ cochleae, total levels of MIIC were slightly increased (Figure 6N), whereas total MIIA levels were similar compared to controls (Figure 6O). Taken together, reduced junctional localization of MIIB, MIIC, and pRLC and the absence of MIIB and MIIA in apical foci in *Ptk7*$^{-/-}$ OC suggest that *Ptk7* regulates myosin II activity.

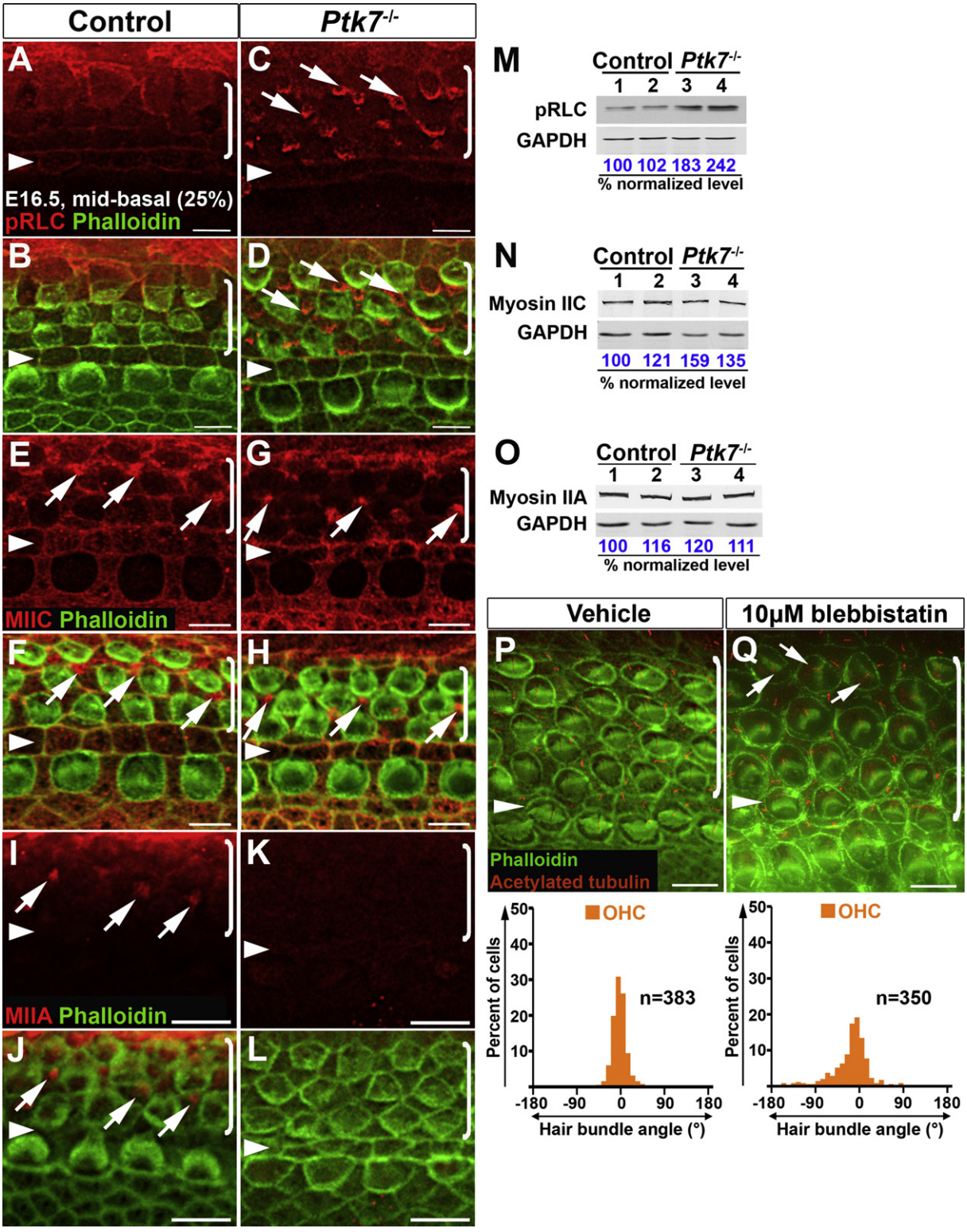

Figure 6. *Ptk7* Regulates Myosin II Activity to Orient Hair Cell PCP

(A–L) Localization of pRLC (A–D), MIIC (E–H), and MIIA (I–L) in the midbasal region of OC (25% cochlear length) at E16.5. Green, phalloidin staining.
(A and B) In the control, pRLC (red) is localized to cell-cell contacts.
(C and D) In *Ptk7*$^{-/-}$ OC, pRLC staining was decreased at cell boundaries but increased in apical foci in supporting cells (arrows).
(E and F) In the control, MIIC (red) localizes to cell-cell contacts and apical foci in supporting cells (arrows).
(G and H) In *Ptk7*$^{-/-}$ OC, MIIC staining was reduced at cell boundaries but still localized to apical foci in supporting cells (arrows).
(I and J) In the control, MIIA (red) is localized to apical foci in supporting cells (arrows).
(K and L) In *Ptk7*$^{-/-}$ OC, MIIA staining was undetectable.

If compromised myosin II activity caused bundle misorientation in *Ptk7*$^{-/-}$ mutants, then blocking myosin II activity should result in similar bundle orientation defects. Because MIIA, MIIB, and MIIC are all present and probably function redundantly in the OC, we took a pharmacological approach and applied the myosin II inhibitor blebbistatin to cochlear explant cultures around the time of stereociliary bundle formation (Supplemental Experimental Procedures). We found that explants treated with blebbistatin displayed bundle misorientation (arrows, Figure 6Q), whereas bundle orientation in control explants was relatively normal (Figure 6P). Therefore, we conclude that myosin II activity is required for hair cell PCP.

Ptk7 Promotes Planar Asymmetry of Junctional Vinculin

Defects in myosin II localization suggest that myosin II function is compromised in *Ptk7*$^{-/-}$ OC. To evaluate myosin II function, we examined junctional vinculin localization. Vinculin is a tension-sensitive actin-binding protein involved in anchoring actin filaments to adhesion complexes at both focal adhesions and adherens junctions [35–37]. Recent in vitro studies demonstrate that recruitment of vinculin to adhesion sites is myosin II dependent [38–41]. At E16.5, we observed a base-to-apex gradient of junctional vinculin localization in the control OC that coincides with the gradient of MIIB distribution (see Figures 5A–5E). In the midbasal region of control cochlea, vinculin was asymmetrically localized along cell-cell contacts and enriched on the medial side of hair cell membranes (Figures 7A–7C). Strikingly, in the midbasal region of the *Ptk7*$^{-/-}$ OC, planar asymmetry of junctional vinculin was abolished, and overall junctional vinculin staining was reduced compared to controls (Figures 7D–7F). On the other hand, localization of resident adherens junction proteins, including E-cadherin and β-catenin, was comparable to controls (Figure S4), suggesting that loss of vinculin planar asymmetry in *Ptk7*$^{-/-}$ OC is not a result of disrupted adherens junctions. In the apex, junctional vinculin staining in control and *Ptk7*$^{-/-}$ OC was similar and both lacked apparent planar asymmetry (Figures 7G–7J). These results indicate that *Ptk7* promotes planar asymmetry of junctional vinculin and strongly support the hypothesis that *Ptk7* regulates myosin II-based polarized contractile forces between OC epithelial cells.

Planar Asymmetry of Junctional Vinculin Is Restored in *Fz3*$^{-/-}$;*Ptk7*$^{-/-}$ Mutants

In *Ptk7* mutants, loss of vinculin planar asymmetry correlated with bundle misorientation. To further understand the functional significance of vinculin planar asymmetry as well as the basis for the suppression of the *Ptk7* bundle orientation phenotype by *Fz3* (see Figure 2), we examined vinculin localization in *Fz3*$^{-/-}$ and *Fz3*$^{-/-}$;*Ptk7*$^{-/-}$ mutants at E16.5. In the *Fz3*$^{-/-}$ OC, staining intensity of junctional vinculin was similar to controls, though its planar asymmetry appeared less robust (Figures 7K–7M). Remarkably, planar asymmetry of junctional vinculin was restored in *Fz3*$^{-/-}$;*Ptk7*$^{-/-}$ mutants (Figures 7N–7P). Moreover, *Fz3*$^{-/-}$;*Ptk7*$^{-/-}$ double mutants showed an increase in junctional MIIB levels and reappearance of apical MIIB foci in supporting cells compared to *Ptk7* single mutants (Figure S4). Taken together, these results demonstrate a strong correlation between vinculin planar asymmetry and hair cell PCP and further suggest that *Ptk7* and *Fz3* act in an opposing fashion to regulate contractile forces between OC epithelial cells.

Discussion

In this study, we present multiple lines of evidence that *Ptk7* is not an obligatory component of the noncanonical Wnt pathway; rather, during PCP signaling in the auditory epithelium, *Ptk7* and the noncanonical Wnt pathway differentially regulate myosin II-based contractile forces to orient PCP. Furthermore, we uncover an active role of supporting cells in this process through a contractile apical myosin II network (Figure 7Q).

In the mouse, *Ptk7* is not required for membrane recruitment of Dvl2 either in the inner ear (this study) or in the mesoderm during gastrulation [15]. These results contradict studies in *Xenopus*, where it has been shown that *Ptk7* mediates membrane recruitment of Dishevelled through a PKCδ-dependent mechanism [13, 14]. A possible explanation is that the *Xenopus* Dishevelled membrane recruitment assay was based on exogenously expressed Dishevelled, whereas we examined endogenous Dvl2 in the mouse. There is also evidence that PTK7 may have evolved different functions in mice and *Xenopus*. For example, PTK7 has been shown to regulate neural crest migration in *Xenopus* but not in mice [12, 13]. Although it is formally possible that PTK7 might mediate membrane localization of other mouse Dishevelled proteins (Dvl1 and Dvl3), it is unlikely to be the primary function of PTK7 in PCP regulation in the OC. Instead, our results strongly support a function of PTK7 in myosin II regulation to align PCP.

Interestingly, bundle misorientation in *Ptk7* mutants is largely restricted to OHC3 despite broad expression of PTK7 in the cochlea. OHC3s are positioned at the lateral edge of the OC and, as such, are mechanically coupled to a different group of cells than the other hair cell rows. We speculate that their unique mechanical environment may render OHC3s more sensitive to compromised myosin II function in *Ptk7* mutants. Furthermore, normal Dvl2 localization suggests that the noncanonical Wnt pathway is at least partially active in *Ptk7* mutants. We propose that overall PCP signaling is weakened but not disrupted in *Ptk7* mutants, resulting in defects only in OHC3s.

Our genetic analysis revealed, rather surprisingly, opposing effects of *Ptk7* and *Fz3*/*Fz6* on stereociliary bundle orientation. These findings contrast with our earlier observation that *Ptk7* and *Vangl2*^{Lp} mutations showed a positive genetic interaction such that double heterozygous animals displayed spina bifida [8]. It is worth noting that an allelic series of *Vangl2* mutations caused neural tube defects ranging from mild (e.g., spina bifida) to severe (e.g., craniorachischisis) in both mice and humans [42–44]. Thus, reduced *Ptk7* gene dosage may

(M–O) Western blot analysis of total levels of pRLC, MIIC, and MIIA in E16.5 *Ptk7*$^{-/-}$ cochleae. Lysates from four cochleae of the same genotype were pooled and loaded in each lane. GAPDH served as loading control. Numbers on the bottom indicate percentage of normalized levels.
(P and Q) Phalloidin (green) and acetylated-tubulin (red) staining of cochlear explants treated with either vehicle (P) or 10 μM blebbistatin (Q), with quantification of bundle orientation shown beneath.
Arrows indicate examples of misoriented stereociliary bundles in blebbistatin-treated explants. Arrowheads indicate the row of pillar cells. Brackets indicate OHC rows. Lateral is up in all micrographs. Scale bars represent 5 μm in (A)–(H) and 6 μm in (I)–(L) and (P)–(Q).

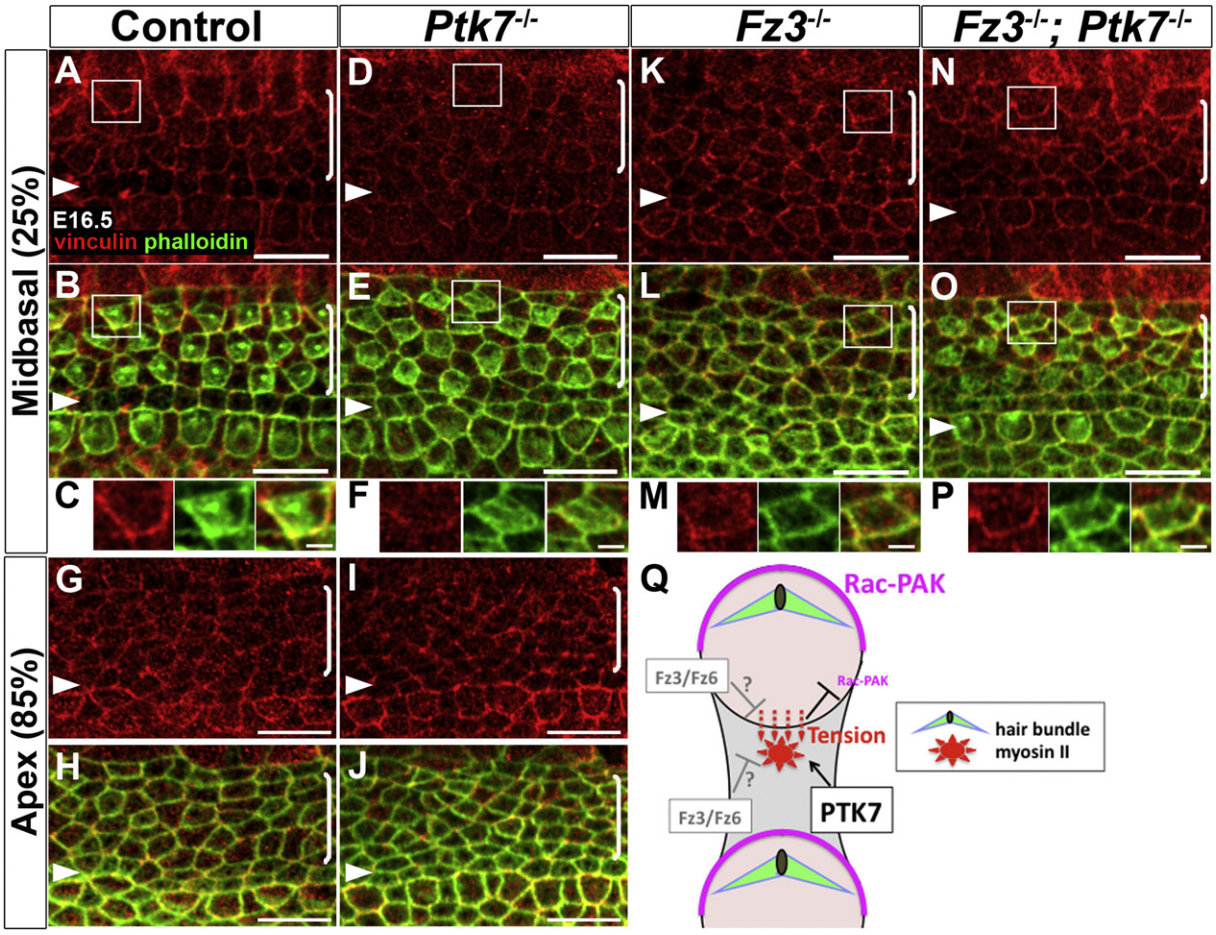

Figure 7. Planar Asymmetry of Junctional Vinculin Is Abolished in *Ptk7*$^{-/-}$ OC and Restored in *Fz3*$^{-/-}$;*Ptk7*$^{-/-}$ OC

(A–P) Confocal images of vinculin (red) and phalloidin (green) staining at E16.5.

(A–C) In the midbasal region (25% cochlear length) of control OC, vinculin was asymmetrically localized along cell-cell junctions and enriched on the medial side of hair cell membranes.

(D–F) In the midbasal region of *Ptk7*$^{-/-}$ OC, junctional vinculin localization lost planar asymmetry and was greatly reduced compared to controls.

(G–J) In the apex (85% cochlear length), junctional vinculin staining in the control (G, H) and *Ptk7*$^{-/-}$ (I, J) OC was similar, with no apparent planar asymmetry.

(K–M) In the midbasal region of *Fz3*$^{-/-}$ OC, junctional vinculin staining was similar to controls but its planar asymmetry was less robust.

(N–P) In the midbasal region of the *Fz3*$^{-/-}$;*Ptk7*$^{-/-}$ OC, planar asymmetry of junctional vinculin was restored.

(C, F, M, P) High magnification of the boxed hair cell above.

Lateral is up in all micrographs. Scale bars represent 2 μm in (C), (F), (M), and (P) and 10 μm in other panels.

(Q) A proposed model for regulation of hair cell PCP by *Ptk7*. Acting in supporting cells (shaded gray), *Ptk7* mediates the assembly of a contractile apical myosin II network to exert pulling forces on the medial border of hair cells, leading to enhanced contractile tension as evidenced by increased vinculin recruitment. In turn, polarized contractile tension promotes asymmetric Rac-PAK activity on the lateral side of hair cell cortex (shown in magenta) to orient the stereociliary bundle. *Fz3/Fz6* may act in hair cells and/or supporting cells to counterbalance *Ptk7*-mediated contractile tension on hair cells.

See also Figure S4.

enhance the dominant effects of the *Looptail* mutation on neural tube closure. *Fz3/Fz6* genes have unique qualities among the noncanonical Wnt pathway components: *Fz3/Fz6* mutations cause bundle misorientation primarily in IHCs, where bundle orientation is frequently reversed. Furthermore, Fz3/Fz6 and Dvl2 appear to localize to opposite poles of hair cells, which is at odds with a conserved role of Fz in Dishevelled recruitment through direct binding [45]. Thus, our results add to a growing body of evidence that suggests *Fz3/Fz6* use novel mechanisms to regulate hair cell PCP. We propose that *Fz3/Fz6* and *Ptk7* act in an opposing fashion to modulate actomyosin contractility in the OC and that reduced Fz3 localization in the *Ptk7*$^{-/-}$ OC is probably a secondary effect of altered actomyosin organization rather than the cause for bundle misorientation.

We show that *Ptk7* and the noncanonical Wnt pathway differentially regulate a contractile apical myosin II network in supporting cells. These structures are analogous to those observed during *Drosophila* gastrulation [46, 47] and germ band extension [48–50], which generate pulsed contractile forces near cell-cell junctions to drive apical constriction and cell intercalation, respectively. We hypothesize that the apical myosin II foci in supporting cells may engage in similar contractile behaviors to exert pulling forces on neighboring hair cells. *Ptk7* modulates myosin II-based contractile tension on hair cells by mediating the assembly of the apical myosin network in supporting cells. *Fz3/Fz6* may modulate contractility in hair cells and/or supporting cells to counterbalance the pulling forces on hair cells (Figure 7Q). In support of this model, we show that vinculin, a force-sensitive actin binding

molecule, is normally enriched along the medial junctions of hair cells, that this planar asymmetry is lost in *Ptk7*$^{-/-}$ mutants, and importantly, that both vinculin planar asymmetry and bundle orientation were restored in *Fz3*$^{-/-}$;*Ptk7*$^{-/-}$ double mutants.

The precise mechanisms by which PTK7 regulates myosin II activity remain to be determined. Paradoxically, in spite of reduced junctional myosin II staining, pRLC level was increased in *Ptk7*$^{-/-}$ OC. Therefore, it is unlikely that PTK7 regulates myosin II activity through RLC phosphorylation per se. Different myosin II isoforms are regulated by distinct upstream signals [51]. *Ptk7* deficiency affected the localization of all three heavy chain isoforms, with the strongest impact on MIIB, which has properties best suited to exert tension [33]. These results are consistent with a role of PTK7 in myosin II heavy chain regulation. We suspect that the increased level of pRLC in *Ptk7*$^{-/-}$ OC may reflect a compensatory response to compromised myosin II heavy chain function.

How might contractile tension orient hair cell PCP? We showed previously that hair cell PCP is controlled by Rac-PAK signaling [4, 5]. Interestingly, several in vitro studies suggest that tension and myosin II can inhibit Rac activity through GEFs and GAPs for Rac [52–55]. Consistent with this idea, activated PAK and vinculin exhibit complementary patterns of planar asymmetry in hair cells. We propose that polarized contractile tension between OC epithelial cells regulates the spatial pattern of Rac-PAK activity to orient hair cell PCP (Figure 7Q).

Supplemental Information

Supplemental Information includes Supplemental Experimental Procedures and four figures and can be found with this article online at doi:10.1016/j.cub.2012.03.068.

Acknowledgments

We thank Paul Adler, Douglas DeSimone, Alan “Rick” Horwitz, Raymond Keller, Martin Schwartz, Ann Sutherland, and members of the X.L. laboratory for helpful comments on the manuscript; Robert Adelstein and Matthew Kelley for *Myh10*^{DN} mice; and Jeremy Nathans and Yanshu Wang for Fz plasmids, antibodies, and mice. This study was supported by a Basil O’Connor Starter Scholar Research Awards (#5-FY07-166) from the March of Dimes Foundation and the NIH grant R01 DC009238 (to X.L.). C.W.S. was supported by NIH training grant T32 GM008136 for Cell and Molecular Biology at the University of Virginia.

Received: December 7, 2011
Revised: March 12, 2012
Accepted: March 27, 2012
Published online: May 3, 2012

References

1. Schwander, M., Kachar, B., and Müller, U. (2010). Review series: The cell biology of hearing. J. Cell Biol. *190*, 9–20.
2. Goodrich, L.V., and Strutt, D. (2011). Principles of planar polarity in animal development. Development *138*, 1877–1892.
3. Rida, P.C., and Chen, P. (2009). Line up and listen: Planar cell polarity regulation in the mammalian inner ear. Semin. Cell Dev. Biol. *20*, 978–985.
4. Grimsley-Myers, C.M., Sipe, C.W., Géléoc, G.S., and Lu, X. (2009). The small GTPase Rac1 regulates auditory hair cell morphogenesis. J. Neurosci. *29*, 15859–15869.
5. Sipe, C.W., and Lu, X. (2011). Kif3a regulates planar polarization of auditory hair cells through both ciliary and non-ciliary mechanisms. Development *138*, 3441–3449.
6. Yamamoto, N., Okano, T., Ma, X., Adelstein, R.S., and Kelley, M.W. (2009). Myosin II regulates extension, growth and patterning in the mammalian cochlear duct. Development *136*, 1977–1986.
7. Montcouquiol, M., Rachel, R.A., Lanford, P.J., Copeland, N.G., Jenkins, N.A., and Kelley, M.W. (2003). Identification of Vangl2 and Scrb1 as planar polarity genes in mammals. Nature *423*, 173–177.
8. Lu, X., Borchers, A.G., Jolicoeur, C., Rayburn, H., Baker, J.C., and Tessier-Lavigne, M. (2004). PTK7/CCK-4 is a novel regulator of planar cell polarity in vertebrates. Nature *430*, 93–98.
9. Narimatsu, M., Bose, R., Pye, M., Zhang, L., Miller, B., Ching, P., Sakuma, R., Luga, V., Roncari, L., Attisano, L., and Wrana, J.L. (2009). Regulation of planar cell polarity by Smurf ubiquitin ligases. Cell *137*, 295–307.
10. Merte, J., Jensen, D., Wright, K., Sarsfield, S., Wang, Y., Schekman, R., and Ginty, D.D. (2010). Sec24b selectively sorts Vangl2 to regulate planar cell polarity during neural tube closure. Nat. Cell Biol. *12*, 41–46, 1–8.
11. Wansleeben, C., Feitsma, H., Montcouquiol, M., Kroon, C., Cuppen, E., and Meijlink, F. (2010). Planar cell polarity defects and defective Vangl2 trafficking in mutants for the COPII gene Sec24b. Development *137*, 1067–1073.
12. Paudyal, A., Damrau, C., Patterson, V.L., Ermakov, A., Formstone, C., Lalanne, Z., Wells, S., Lu, X., Norris, D.P., Dean, C.H., et al. (2010). The novel mouse mutant, chuzhoi, has disruption of Ptk7 protein and exhibits defects in neural tube, heart and lung development and abnormal planar cell polarity in the ear. BMC Dev. Biol. *10*, 87.
13. Shnitsar, I., and Borchers, A. (2008). PTK7 recruits dsh to regulate neural crest migration. Development *135*, 4015–4024.
14. Wehner, P., Shnitsar, I., Urlaub, H., and Borchers, A. (2011). RACK1 is a novel interaction partner of PTK7 that is required for neural tube closure. Development *138*, 1321–1327.
15. Yen, W.W., Williams, M., Periasamy, A., Conaway, M., Burdsal, C., Keller, R., Lu, X., and Sutherland, A. (2009). PTK7 is essential for polarized cell motility and convergent extension during mouse gastrulation. Development *136*, 2039–2048.
16. Adler, P.N. (2002). Planar signaling and morphogenesis in *Drosophila*. Dev. Cell *2*, 525–535.
17. Axelrod, J.D. (2001). Unipolar membrane association of Dishevelled mediates Frizzled planar cell polarity signaling. Genes Dev. *15*, 1182–1187.
18. Wang, J., Mark, S., Zhang, X., Qian, D., Yoo, S.J., Radde-Gallwitz, K., Zhang, Y., Lin, X., Collazo, A., Wynshaw-Boris, A., and Chen, P. (2005). Regulation of polarized extension and planar cell polarity in the cochlea by the vertebrate PCP pathway. Nat. Genet. *37*, 980–985.
19. Wang, Y., Guo, N., and Nathans, J. (2006). The role of Frizzled3 and Frizzled6 in neural tube closure and in the planar polarity of inner-ear sensory hair cells. J. Neurosci. *26*, 2147–2156.
20. Montcouquiol, M., Sans, N., Huss, D., Kach, J., Dickman, J.D., Forge, A., Rachel, R.A., Copeland, N.G., Jenkins, N.A., Bogani, D., et al. (2006). Asymmetric localization of Vangl2 and Fz3 indicate novel mechanisms for planar cell polarity in mammals. J. Neurosci. *26*, 5265–5275.
21. Hébert, J.M., and McConnell, S.K. (2000). Targeting of cre to the Foxg1 (BF-1) locus mediates loxP recombination in the telencephalon and other developing head structures. Dev. Biol. *222*, 296–306.
22. Lakso, M., Pichel, J.G., Gorman, J.R., Sauer, B., Okamoto, Y., Lee, E., Alt, F.W., and Westphal, H. (1996). Efficient in vivo manipulation of mouse genomic sequences at the zygote stage. Proc. Natl. Acad. Sci. USA *93*, 5860–5865.
23. Boutros, M., Paricio, N., Strutt, D.I., and Mlodzik, M. (1998). Dishevelled activates JNK and discriminates between JNK pathways in planar polarity and wingless signaling. Cell *94*, 109–118.
24. Yamanaka, H., Moriguchi, T., Masuyama, N., Kusakabe, M., Hanafusa, H., Takada, R., Takada, S., and Nishida, E. (2002). JNK functions in the non-canonical Wnt pathway to regulate convergent extension movements in vertebrates. EMBO Rep. *3*, 69–75.
25. Dong, C., Yang, D.D., Wysk, M., Whitmarsh, A.J., Davis, R.J., and Flavell, R.A. (1998). Defective T cell differentiation in the absence of Jnk1. Science *282*, 2092–2095.
26. Kuan, C.Y., Yang, D.D., Samanta Roy, D.R., Davis, R.J., Rakic, P., and Flavell, R.A. (1999). The Jnk1 and Jnk2 protein kinases are required for regional specific apoptosis during early brain development. Neuron *22*, 667–676.
27. Davis, R.J. (2000). Signal transduction by the JNK group of MAP kinases. Cell *103*, 239–252.

28. Winter, C.G., Wang, B., Ballew, A., Royou, A., Karess, R., Axelrod, J.D., and Luo, L. (2001). *Drosophila* Rho-associated kinase (Drok) links Frizzled-mediated planar cell polarity signaling to the actin cytoskeleton. Cell *105*, 81–91.
29. Lee, J.Y., Marston, D.J., Walston, T., Hardin, J., Halberstadt, A., and Goldstein, B. (2006). Wnt/Frizzled signaling controls *C. elegans* gastrulation by activating actomyosin contractility. Curr. Biol. *16*, 1986–1997.
30. Conti, M.A., and Adelstein, R.S. (2008). Nonmuscle myosin II moves in new directions. J. Cell Sci. *121*, 11–18.
31. Skoglund, P., Rolo, A., Chen, X., Gumbiner, B.M., and Keller, R. (2008). Convergence and extension at gastrulation require a myosin IIB-dependent cortical actin network. Development *135*, 2435–2444.
32. Rolo, A., Skoglund, P., and Keller, R. (2009). Morphogenetic movements driving neural tube closure in *Xenopus* require myosin IIB. Dev. Biol. *327*, 327–338.
33. Vicente-Manzanares, M., Ma, X., Adelstein, R.S., and Horwitz, A.R. (2009). Non-muscle myosin II takes centre stage in cell adhesion and migration. Nat. Rev. Mol. Cell Biol. *10*, 778–790.
34. Ma, X., Bao, J., and Adelstein, R.S. (2007). Loss of cell adhesion causes hydrocephalus in nonmuscle myosin II-B-ablated and mutated mice. Mol. Biol. Cell *18*, 2305–2312.
35. Peng, X., Nelson, E.S., Maiers, J.L., and DeMali, K.A. (2011). New insights into vinculin function and regulation. Int. Rev. Cell Mol. Biol. *287*, 191–231.
36. Hoffman, B.D., Grashoff, C., and Schwartz, M.A. (2011). Dynamic molecular processes mediate cellular mechanotransduction. Nature *475*, 316–323.
37. Gomez, G.A., McLachlan, R.W., and Yap, A.S. (2011). Productive tension: force-sensing and homeostasis of cell-cell junctions. Trends Cell Biol. *21*, 499–505.
38. Pasapera, A.M., Schneider, I.C., Rericha, E., Schlaepfer, D.D., and Waterman, C.M. (2010). Myosin II activity regulates vinculin recruitment to focal adhesions through FAK-mediated paxillin phosphorylation. J. Cell Biol. *188*, 877–890.
39. Grashoff, C., Hoffman, B.D., Brenner, M.D., Zhou, R., Parsons, M., Yang, M.T., McLean, M.A., Sligar, S.G., Chen, C.S., Ha, T., and Schwartz, M.A. (2010). Measuring mechanical tension across vinculin reveals regulation of focal adhesion dynamics. Nature *466*, 263–266.
40. Yonemura, S., Wada, Y., Watanabe, T., Nagafuchi, A., and Shibata, M. (2010). alpha-Catenin as a tension transducer that induces adherens junction development. Nat. Cell Biol. *12*, 533–542.
41. le Duc, Q., Shi, Q., Blonk, I., Sonnenberg, A., Wang, N., Leckband, D., and de Rooij, J. (2010). Vinculin potentiates E-cadherin mechanosensing and is recruited to actin-anchored sites within adherens junctions in a myosin II-dependent manner. J. Cell Biol. *189*, 1107–1115.
42. Kibar, Z., Salem, S., Bosoi, C.M., Pauwels, E., De Marco, P., Merello, E., Bassuk, A.G., Capra, V., and Gros, P. (2011). Contribution of VANGL2 mutations to isolated neural tube defects. Clin. Genet. *80*, 76–82.
43. Guyot, M.C., Bosoi, C.M., Kharfallah, F., Reynolds, A., Drapeau, P., Justice, M., Gros, P., and Kibar, Z. (2011). A novel hypomorphic Looptail allele at the planar cell polarity Vangl2 gene. Dev. Dyn. *240*, 839–849.
44. Yin, H., Copley, C.O., Goodrich, L.V., and Deans, M.R. (2012). Comparison of phenotypes between different vangl2 mutants demonstrates dominant effects of the Looptail mutation during hair cell development. PLoS ONE *7*, e31988.
45. Wong, H.C., Bourdelas, A., Krauss, A., Lee, H.J., Shao, Y., Wu, D., Mlodzik, M., Shi, D.L., and Zheng, J. (2003). Direct binding of the PDZ domain of Dishevelled to a conserved internal sequence in the C-terminal region of Frizzled. Mol. Cell *12*, 1251–1260.
46. Martin, A.C., Kaschube, M., and Wieschaus, E.F. (2009). Pulsed contractions of an actin-myosin network drive apical constriction. Nature *457*, 495–499.
47. Martin, A.C., Gelbart, M., Fernandez-Gonzalez, R., Kaschube, M., and Wieschaus, E.F. (2010). Integration of contractile forces during tissue invagination. J. Cell Biol. *188*, 735–749.
48. Rauzi, M., Lenne, P.F., and Lecuit, T. (2010). Planar polarized actomyosin contractile flows control epithelial junction remodelling. Nature *468*, 1110–1114.
49. Fernandez-Gonzalez, R., and Zallen, J.A. (2011). Oscillatory behaviors and hierarchical assembly of contractile structures in intercalating cells. Phys. Biol. *8*, 045005.
50. Sawyer, J.K., Choi, W., Jung, K.C., He, L., Harris, N.J., and Peifer, M. (2011). A contractile actomyosin network linked to adherens junctions by Canoe/afadin helps drive convergent extension. Mol. Biol. Cell *22*, 2491–2508.
51. Smutny, M., Cox, H.L., Leerberg, J.M., Kovacs, E.M., Conti, M.A., Ferguson, C., Hamilton, N.A., Parton, R.G., Adelstein, R.S., and Yap, A.S. (2010). Myosin II isoforms identify distinct functional modules that support integrity of the epithelial zonula adherens. Nat. Cell Biol. *12*, 696–702.
52. Katsumi, A., Milanini, J., Kiosses, W.B., del Pozo, M.A., Kaunas, R., Chien, S., Hahn, K.M., and Schwartz, M.A. (2002). Effects of cell tension on the small GTPase Rac. J. Cell Biol. *158*, 153–164.
53. Lee, C.S., Choi, C.K., Shin, E.Y., Schwartz, M.A., and Kim, E.G. (2010). Myosin II directly binds and inhibits Dbl family guanine nucleotide exchange factors: a possible link to Rho family GTPases. J. Cell Biol. *190*, 663–674.
54. Even-Ram, S., Doyle, A.D., Conti, M.A., Matsumoto, K., Adelstein, R.S., and Yamada, K.M. (2007). Myosin IIA regulates cell motility and actomyosin-microtubule crosstalk. Nat. Cell Biol. *9*, 299–309.
55. Ehrlicher, A.J., Nakamura, F., Hartwig, J.H., Weitz, D.A., and Stossel, T.P. (2011). Mechanical strain in actin networks regulates FilGAP and integrin binding to filamin A. Nature *478*, 260–263.